Int J Adv Manuf Technol (2014) 74:383–392
DOI 10.1007/s00170-014-6003-4

ORIGINAL ARTICLE

Analysis and porthole die design for a multi-hole extrusion process of a hollow, thin-walled aluminum profile

Liang Chen · Guoqun Zhao · Junquan Yu · Wendong Zhang · Tao Wu

Received: 12 January 2014 / Accepted: 22 May 2014 / Published online: 1 June 2014

Abstract The appropriate die design for multi-hole extrusion is still a challenging task because of the complicated circumstances and large material deformation during extrusion process. In the present study, the material flow during multi-hole extrusion process for producing a hollow and thin-walled profile was revealed by means of numerical simulation based on the Arbitrary Lagrangian Eulerian (ALE) method. The effects of eccentricity ratio, shape of the second-step welding chamber, and uneven bearing length on the exit velocity distribution of extrudate were synthetically investigated, and a two-hole porthole die was designed accordingly. The exit velocity and temperature on the extrudate in this optimized die were analyzed and compared with the initial die, and it was found that both of them exhibit better uniformity, which is beneficial for the enhancement of product quality. Through performing the current work, a logical and effective route for designing multi-hole porthole die was proposed as the guidance for die designers.

Keywords Multi-hole extrusion · Thin-walled profile · Material flow · Die design

1 Introduction

The porthole die has been widely applied for the extrusion of hollow profiles due to its advantages in producing complex cross section and low manufacturing cost [1]. In recent years, with the rapid development of extruder and increasing demand in high productivity, the multi-hole porthole die extrusion becomes feasible and desiderate. For multi-hole extrusion, it could produce several extrudate in one process cycle resulting in a substantial enhancement of the productivity. Besides, the required extrusion force is much lower for a given billet and profile. Therefore, the development of multi-hole extrusion process has attracted much attention from researchers [2].

The extrusion die plays an important role in single-hole or multi-hole extrusion process, since it strongly affects the homogeneity of material flow inside the die. A well-designed die should have a favorable material flow behavior to guarantee that the velocity distribution in the cross section of the extrudate is homogeneous. Otherwise, it might cause some defects to the final products, such as twist, wave, and curve and influences the homogeneity of microstructure after cooling and heat treatment [3–5]. Theoretically, the die design scheme should be constructed based on a deep understanding of the material flow, the fields of velocity and temperature, and the stress and strain distribution inside the die [6–8]. However, such kind of information is difficult to be obtained because of the complicated circumstances and large material deformation during the extrusion process. And the current die design is still mainly based on the experience and follows the "trial and error" route [9]. After the manufacturing of die, several modifications are still needed to be carried out according to the information fed back from practical production, which causes additional cost and waste of time.

Owing to the rapid development of numerical technology, many researchers have performed some simulation work on aluminum alloy extrusion to provide accurate and theoretical guidance for die design. Lof [10] proposed a new approach for simulating the extrusion process of complex profiles and the simulated results for a particular porthole die show good agreement with the overall process characteristics. Wu [7] developed an optimization system, combining the finite element method (FEM), a polynomial network, and a genetic

L. Chen (✉) · G. Zhao (✉) · J. Yu · W. Zhang · T. Wu
Key Laboratory for Liquid-Solid Structural Evolution and Processing of Materials (Ministry of Education), Shandong University, Jinan, Shandong 250061, People's Republic of China
e-mail: chenliang@sdu.edu.cn
e-mail: zhaogq@sdu.edu.cn

algorithm, for the design of extrusion die. The die geometry was optimized by an improved genetic algorithm based on the data of extrusion force and die deformation obtained from FEM analysis. Jo [11] performed non-steady-state FEM analysis and experiments to investigate the material flow and extrusion force with respect of different process parameters. Fang [12, 13] studied the pocket die extrusion process and evaluated the effects of pocket and bearing length on extrudate temperature, velocity distribution, and extrusion force. The shape parameters of pocket and bearing length were found to be an effective factor on adjusting the metal flow and extrudate temperature, which were verified experimentally. Kathirgamanathan [14] also did similar work by means of DEFORM-3D. Chen [15] carried out 3D FEM simulation on the extrusion process of a large aluminum profile and modified the porthole die by reducing the area of porthole, introducing baffle plate, and adjusting the length of bearing to obtain a more homogeneous distribution of flowing velocity and temperature of extrudate. Li [16] studied the effect of inner cone punch on metal flow in extrusion process using numerical simulation and experiment. Zhang [17] investigated the material flow behavior at each stage during the one extrusion cycle using steady-state finite element simulation for a complex hollow profile. Sun [18] optimized the shape and height of the second-step welding chamber for a porthole die producing a condenser tube using response surface method and genetic algorithm based on the steady-state simulation work. The ideal distribution of velocity and temperature of the extrudate in the bearing exit was achieved and the extrudate quality was obviously improved. In the recent decade, because of the advantages in enhancing productivity and reducing extrusion force of multi-hole extrusion process, some researchers have devoted their efforts on the simulation work of such process and made some trials on the optimization of multi-hole die. Peng [19] investigated the influence of the number and distribution of die orifices on material flow pattern and peak extrusion force in multi-hole extrusion for aluminum rod. He [20] compared the extrusion processes using two-hole porthole dies with and without pockets for producing a solid "I"-shaped profile based on FEM simulation and proposed that the pockets in the lower die are beneficial for achieving better material flow, lower extrusion force, and temperature rise. Ulysse [21] presented an upper-boundary method for evaluating the extrusion force and exit velocity during a multi-hole extrusion process of rod extrudate. Guan [22] and Zhang [23] investigated a three-hole porthole extrusion process of aluminum hollow tube by performing steady-state FEM simulation. In their work, it was found that both of the number of portholes and the die orifice layout significantly influence the material flow, extrusion force, and welding pressure.

From the above open literature, the numerical simulation has been proven to be a powerful tool in revealing the extrusion process. However, it should also be noticed that the majority of researchers focused on single-hole extrusion of large, complex profiles, while the research about multi-hole extrusion is still sparse. Moreover, the research concerning with the multi-hole extrusion is limited to a simple solid profile [2, 19–21, 24] and hollow tube [22, 23]. The material flow behaviors and some physical aspects during multi-hole extrusion, especially for thin-walled profiles, are very complicated and still far from being understood, although these are important considerations for die designers.

Therefore, the numerical simulation for two-hole extrusion process to produce a hollow and thin-walled profile was carried out based on the Arbitrary Lagrangian Eulerian (ALE) method using HyperXtrude as the platform in this study. The material flow behavior and deformation mechanism were investigated by analyzing the simulated results. And the effects of the pivotal components of porthole die, such as the location of die orifices, shape of the second-step welding chamber, and uneven bearing length, on velocity distribution of the extrudate in the bearing exit were synthetically studied. The related information of material flow pattern and temperature distribution of extrudate was also discussed in the final section. By such systematic study on multi-hole extrusion, it was aimed to provide a design route of multi-hole porthole die for hollow and thin-walled profiles to die designers.

2 The basic design of two-hole porthole die

The cross section and dimensions of a hollow, thin-walled profile studied in this article is drawn in Fig. 1, which is a typical architectural aluminum alloy profile. The wall thickness is small and unequal, varying from 0.4 to 0.6 mm, and the maximum length in horizontal direction is 25 mm. The area and perimeter of the cross section are 29.44 mm^2 and 137.44 mm, respectively. Qamar [25] proposed the complexity index for a given profile shape in metal extrusion, which can be described as

$$C = 0.95 + 0.05\left(\frac{P_s}{P_0}\right)^{1.5} \quad (1)$$

where P_s is the perimeter of the cross section of profile and P_0 is the perimeter of equivalent circular section having the same area with the profile. A high complexity index of 1.91 for the present profile is calculated according to Eq. (1) due to its thin-walled characteristic, which indicates a high extrusion force requirement and poor homogeneity of material flow. Hence, a two-hole porthole die is more suitable for the purpose of reducing extrusion force and avoiding too high extrusion ratio.

The simplified 3D model of the basic die design is shown in Fig. 2. The upper and lower dies have the same outer

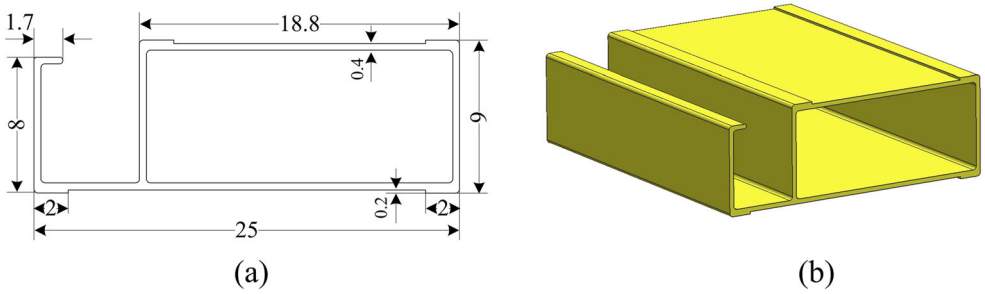

Fig. 1 **a** 2D and **b** 3D geometry of the aluminum alloy profile (unit is in millimeters)

diameter of 158 mm and the same height of 55 mm. Four potholes and two die mandrels were symmetrically designed in the upper die to allocate material rationally and guarantee the same material flow for both extrudate. The width of port bridges in the horizontal and vertical directions is 18 and 12 mm, respectively. The chamfering with an angle of 25° was applied on the port bridges to reduce the resistance of material flow. The lower die consists of a welding chamber, two die orifices, and two-step runout. The welding chamber with a height of 10 mm was used to gather and rejoin the material flowing out from portholes. The part of the rectangular hollow pipe of the profile (Fig. 1) is extruded out between the cuboid-shaped die mandrels and bearing, while the cantilevered part of the profile (Fig. 1) is extruded out from the bearing band directly.

3 Finite element modeling

In the current study, the ALE formulation was utilized to avoid the mesh distortion that emerged in the Lagrangian method and the problems of the free surface tracking that emerged in the Eulerian method [26, 27]. The FEM model for simulating material flow during extrusion was constructed using HyperXtrude, as shown in Fig. 3. The part of porthole was extracted from the model of the upper die shown in Fig. 2a, and the parts of the welding chamber, bearing, and profile were extracted from the lower die shown in Fig. 2b. The very fine tri-prism elements were used to mesh the regions of bearing and profile, since these parts would undergo severe shear deformation. And the element size in the region of the profile is set to be 0.1 mm to have at least four layers in the cross section. The tetrahedral elements were used for the mesh of porthole, welding chamber, and billet, where the element size varies from 0.1 to 6 mm in line with the degree of shear deformation in these regions.

The materials for extrusion billet and dies are Aluminum Alloy 6063 (AA6063) and H13 tool steels, respectively, and the physical properties of both materials are listed in Table 1. The billet was assumed to be visco-plastic, and the tool was assumed to be rigid. The Sellars-Tegart model [10] was adopted to describe the deformation behavior of AA6063 at evaluated temperature. The expression and detailed interpretation of this model have been described in our recent publication [28].

The crucial process parameters used in the present simulation were determined in accordance with the condition in real production, as listed in Table 2. The diameter and length of the cylindrical AA6063 billet are 96 and 192 mm, respectively. The calculated extrusion ratio is around 122.58, which belonged to the scope of quite high extrusion ratio. Because of the thin-walled characteristic and high extrusion ratio, drastic plastic deformation occurs during the extrusion process, which brings about large amount of heat generation and

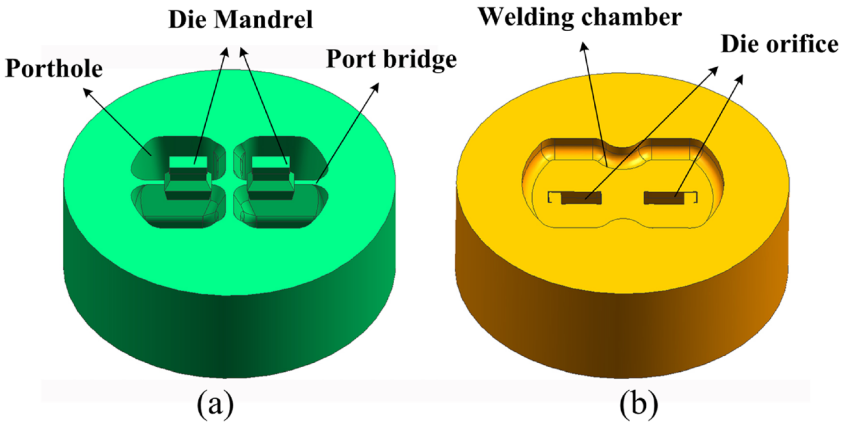

Fig. 2 The basic design of the two-hole porthole die: **a** upper die and **b** lower die

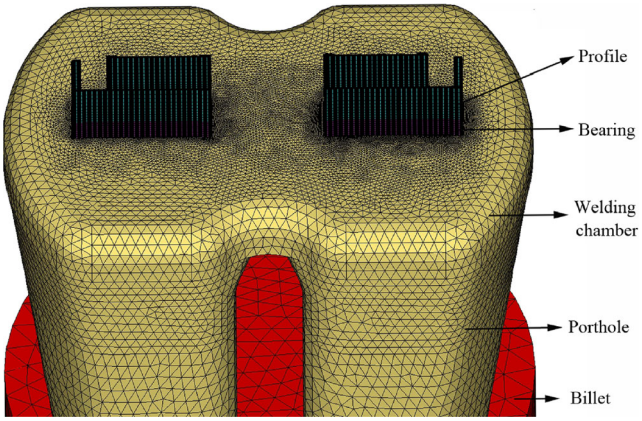

Fig. 3 The finite element model for simulating material flow

thus easily causes a temperature rise in the extrudate, resulting in overburning and other surface defects to the extrudate. Therefore, to avoid such problem, the initial temperature for billet and tools was controlled to be 460 and 430 °C, respectively, and the ram speed is set to be 0.8 mm/s. The heat convection coefficient between the die and billet is assumed to be 3,000 W/m^2 °C. The slop friction is applied on the surfaces in contact with the bearing, while the sticking condition is used for the other interfaces between billet and tools [23, 29].

4 Results and discussion

4.1 Effects of the layout of die orifice on velocity distribution

It has been emphasized that the behavior of material flow during extrusion is a crucial factor on affecting the quality of the final product. Under the condition of nonuniform material flow, the profile is extruded out from the die orifice with a different velocity throughout its cross section, which easily causes twist and bending on the extrudate. Therefore, the uniformity of exit velocity distribution should be highly valued by die designers. In multi-hole extrusion, the location of die orifice is one of the major factors that can affect the exit velocity distribution, which will be discussed in this section. The eccentricity ratio of the die orifice defined in this study

Table 1 The physical properties of AA6063 and H13

	A6063	H13 steel
Density (kg m^3)	2,705	7,870
Thermal conductivity (W/(m K))	231	24.3
Specific heat (J/(kg K))	900	460
Young's modulus (Pa)	4.0e10	2.1e10
Poisson's ratio	0.35	0.35

Table 2 The process parameters used in the present simulation

Billet diameter (mm)	96
Billet length (mm)	192
Initial billet temperature (°C)	460
Initial tool temperature (°C)	430
Extrusion speed (mm/s)	0.8
Heat convection coefficient (W/m^2 °C)	3,000

was modified from the model proposed by Peng [19] and described as

$$e = \frac{b}{a+b} \tag{2}$$

where a is the distance between the die orifice and the wall of the welding chamber and b is the distance between the die orifice and the extrusion center, as schematically shown in Fig. 4. The eccentricity ratio was adjusted from 0.36 to 0.62, and the relevant simulation work was carried out. Additionally, the process parameters, bearing length, and meshing scheme during FEM modeling are kept identical for each case to give a valid comparison.

Figure 5 shows the deformation and velocity distribution of the extrudate for varying eccentricity ratios. It should be firstly pointed out that the distance between the two extrudate shown in Fig. 5 has been adjusted by the authors to give a clear visualization and comparison. Slight asymmetry appears in each case, since the meshes cannot be controlled to be strictly symmetric. With the varying eccentricity ratios, very large velocity difference was overall observed. The maximum velocity difference of 55.87 mm/s emerges when the eccentricity ratio is 0.62, while the minimum velocity difference is 39.03 mm/s for the eccentricity ratio of 0.43. And it should be noticed that the cantilevered part of the extrudate flows much faster than the other regions, since this part was extruded out from the die orifice directly after welding without the resistance resulting from the contact between the material and die mandrel. The large difference in flowing velocity causes a significant twist and bending in the extrudate, especially for the cantilevered part, as shown in Fig. 5.

From Fig. 5, one can also see that with the increase of eccentricity ratio, the velocity of the part near the extrusion center decreases, while the velocity of the cantilevered part of the profile increases. There are two factors mainly responsible for the appearance of this trend. With the increase of eccentricity ratio, the profiles are close to the vertical port bridge. And the retarding effect on material flow resulting from the fiction resistance between the material and vertical port bridge becomes more obvious. However, the cantilevered parts will be far from the porthole wall and its velocity becomes faster due to the reduced effect of friction resistance between the material and the porthole wall. When designing such kind of

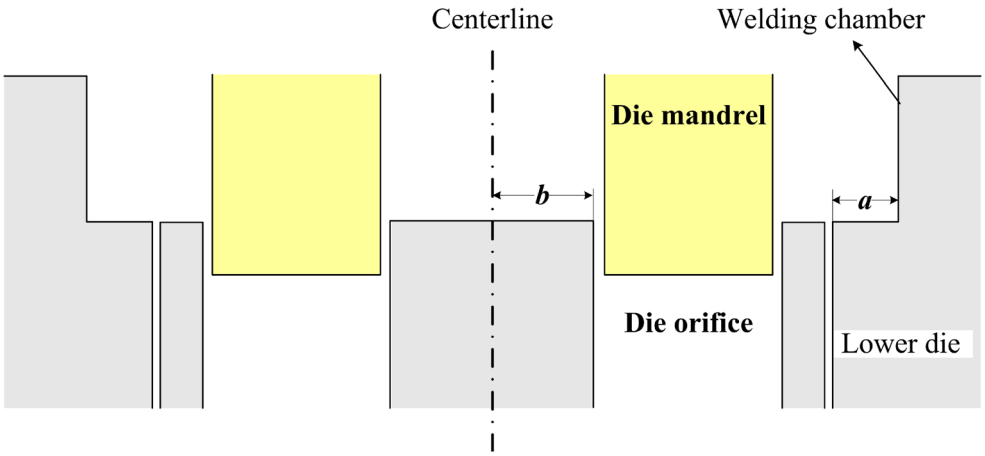

Fig. 4 Schematic drawing of the interpretation of eccentricity ratio (e)

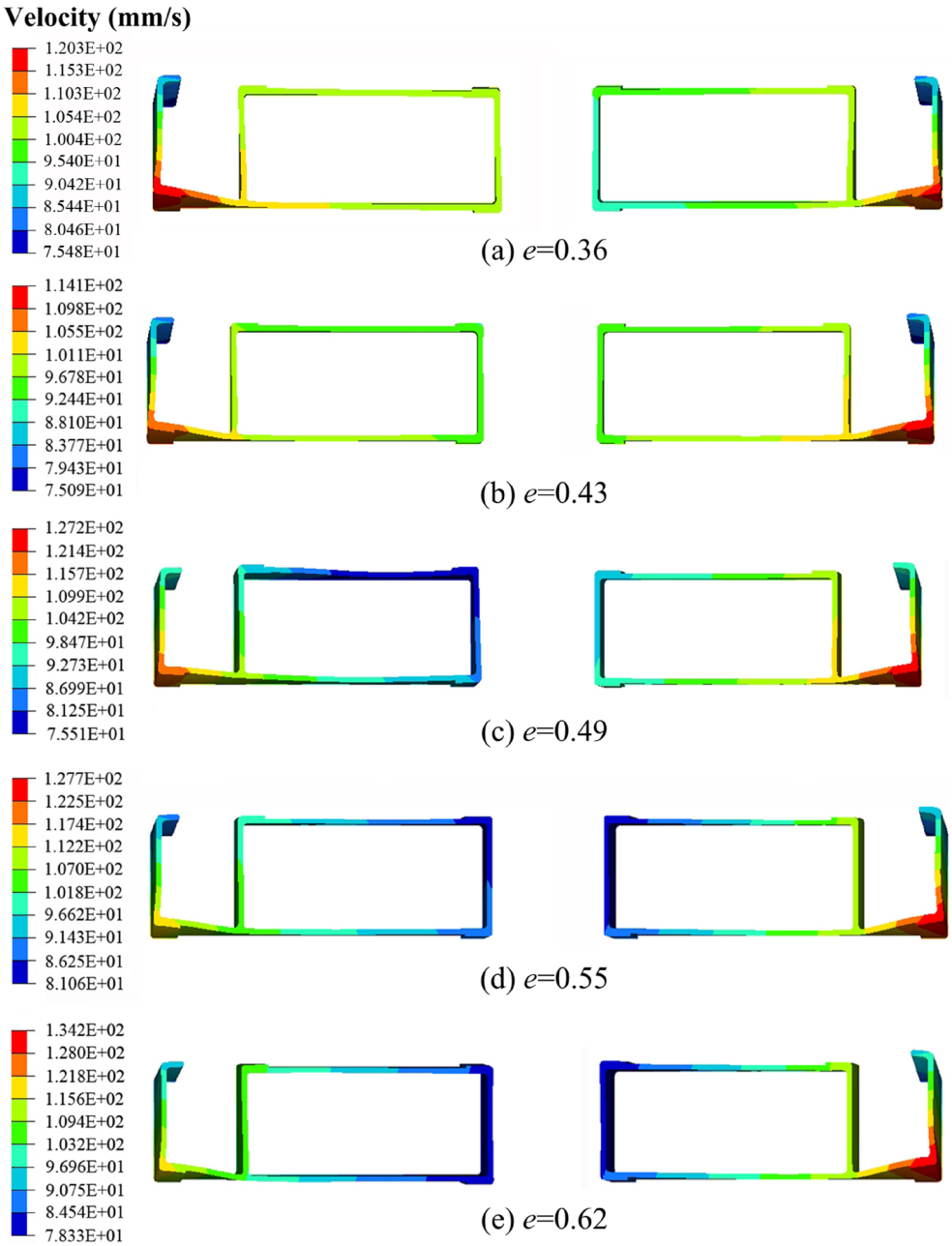

Fig. 5 Velocity distribution of the extrudate with different eccentricity ratios: **a** e=0.36, **b** e=0.43, **c** e=0.49, **d** e=0.55, and **e** e=0.62

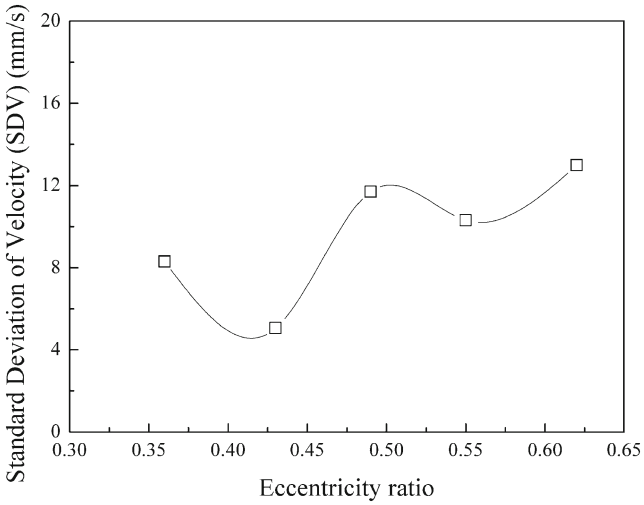

Fig. 6 The SDV values for different eccentricity ratios

multi-hole die, these two factors should be carefully considered. And one proper eccentricity ratio should exist, which can well balance these two factors.

In order to quantitatively evaluate the velocity distribution and to find a proper eccentricity ratio, the standard deviation of the velocity (SDV) was introduced in this study, which is described as

$$\mathrm{SDV} = \sqrt{\frac{\sum_{i=1}^{n}\left(v_i - \overline{\overline{v}}\right)^2}{n}} \tag{3}$$

where n is the total number of the selected nodes, v_i is the axial velocity at node i, and $\overline{\overline{v}}$ is the average velocity for all selected nodes. The velocity information of all the nodes in the cross section of the bearing exit was collected for calculating the values of SDV, and the results are plotted in Fig. 6. It can be seen that the minimum SDV of 5.05 mm/s was obtained when the eccentricity ratio is 0.43. However, in the other cases, all of the SDV values are even higher than 8 mm/s, indicating a poor velocity distribution and severe deformation occurrence on the extrudate. Although the defects of twist and bending on this extrudate cannot be completely avoided only by varying the eccentricity ratio, finding a proper die orifice location is quite important and helpful for the following die modifications. And in the current work, the proper eccentricity ratio was determined to be 0.43.

4.2 Effects of the second-step welding chamber on velocity distribution

The second-step welding chamber has been proven to be effective in controlling the material flow. Moreover, its shape is easier to be modified and machined without any modification on portholes than that of the first-step welding chamber. Hence, it was applied to the present die having the eccentricity ratio of 0.43, and several shapes were designed as illustrated in Fig. 7. The regular rectangle shape was employed, and the distance between the profile and second-step welding chamber was identical for case 1. In cases 2 and 3, the shape was locally modified in some regions, which will be discussed later. The height for both welding chambers is 5 mm to keep the total height identical with the above models.

The velocity distribution of the extrudate for each case is shown in Fig. 8. It can be seen that the material flow becomes even worse for case 1, with a quite high velocity difference of 64.94 mm/s, since an inappropriate shape was designed without considering the velocity difference on the profile. Therefore, some local modifications were carried out in cases 2 and 3, following the principle that the narrow space of the second-step welding chamber was employed in the parts having a relative higher velocity, while a wider space was assigned in the other parts. The maximum velocity has been decreased to 122.4 mm/s for case 2 and 102.8 mm/s for case 3 because of the higher resistance and less material supply due to the narrow space of the second-step welding chamber. On the contrary, the wider space of the second-step welding chamber generates lower resistance and enhances the minimum velocity to 85.66 mm/s for case 2 and 90.0 mm/s for case 3. The

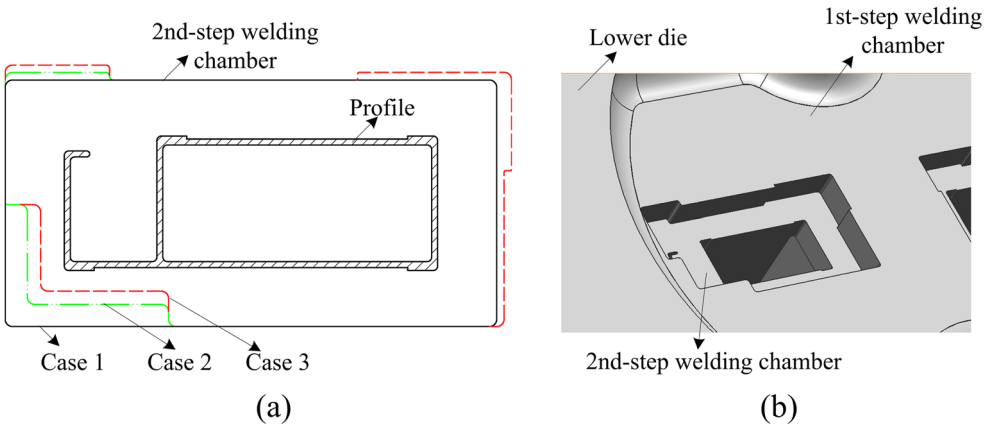

Fig. 7 **a** Three designed shapes for the second-step welding chamber and **b** 3D model of case 3

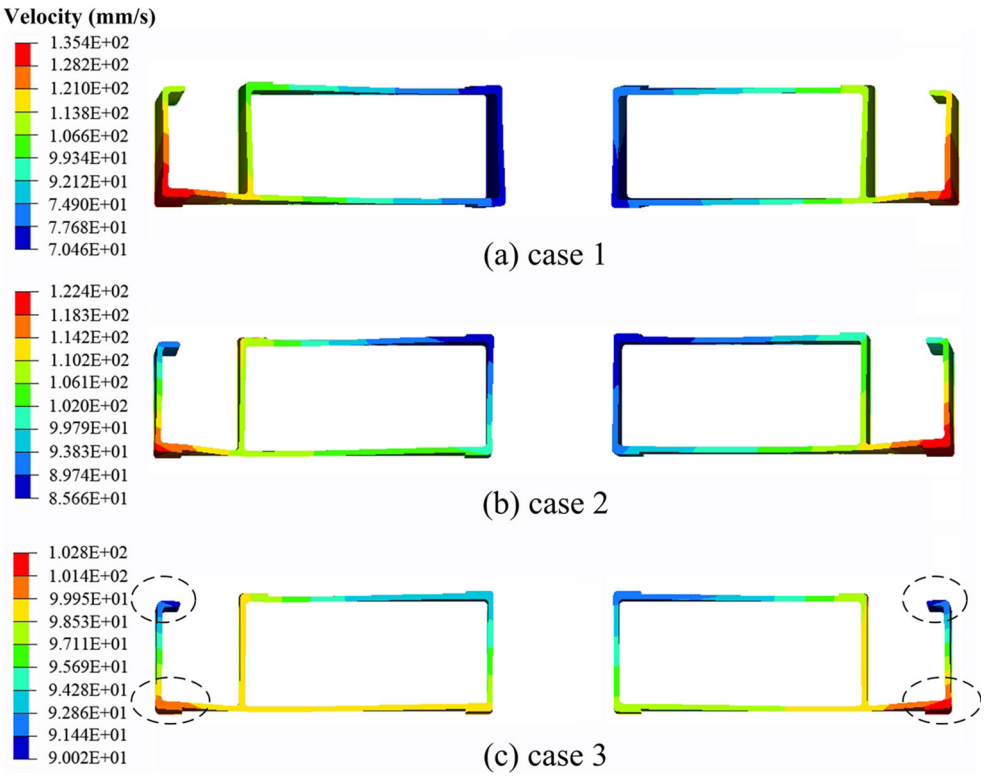

Fig. 8 Velocity distribution of the extrudate for **a** case 1, **b** case 2, and **c** case 3

deformation defects on extrudate are obviously relieved in case 3, and only slight twist defects remain as marked by the dotted circles in Fig. 8c. The calculated SDV significantly decreases from 17.1 mm/s (case 1) to 2.63 mm/s (case 3), as plotted in Fig. 9, indicating that the material flow has been well regulated by the designed second-step welding chamber with appropriate shape.

From the discussion in this section, one can realize that the shape of the second-step welding chamber significantly influences the velocity distribution of the extrudate. A well-designed shape can effectively readjust the material flow to achieve a uniform velocity distribution. And also for the convenience in modification and machining, the second-step welding chamber is recommended to be adopted during the design of a multi-hole extrusion die to improve the product quality.

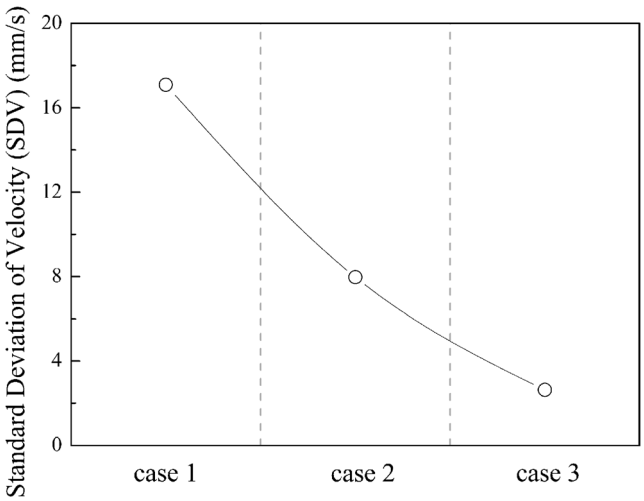

Fig. 9 The SDV values for different shapes of the second-step welding chamber

4.3 Effects of bearing length on velocity distribution

In the above simulation, an identical bearing length of 4 mm was utilized for all the models. However, before the profile is extruded through the die orifice, the friction resistance between the material and die bearing acts as the final "barrier" for material flow. And the uneven bearing length is regularly designed to adjust the material flow in practical production. Therefore, the uneven bearing length was considered in the die with the second-step welding chamber of case 3 and the

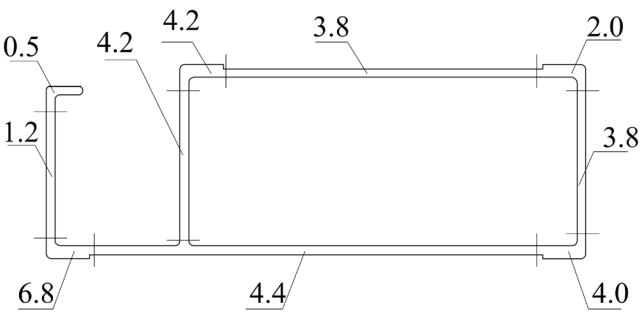

Fig. 10 The assignment of uneven bearing length in profile (unit is in millimeters)

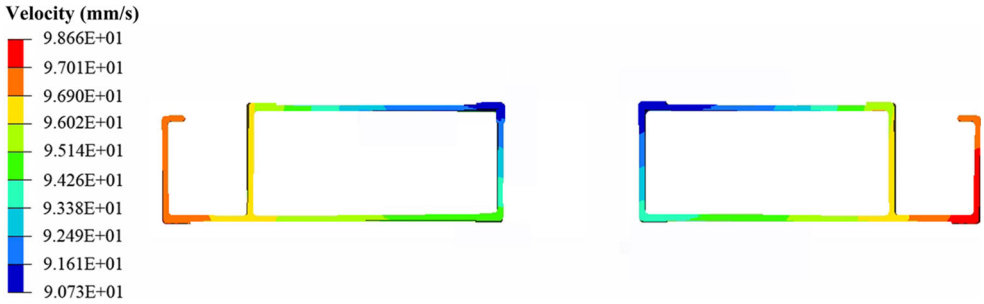

Fig. 11 Velocity distribution of the extrudate with uneven bearing length, the second-step welding chamber, and eccentricity ratio of 0.43

eccentricity ratio of 0.43. According to the information of velocity fed back from Fig. 8c, the bearing length in different regions was adjusted and its effects on exit velocity distribution of extrudate were examined. The proper assignment of uneven bearing length is illustrated in Fig. 10. The longer bearing was applied in the regions having a higher velocity to generate additional friction resistance and thus decrease the exit velocity in the cross section of corresponding regions. On the other hand, a shorter bearing was applied to reduce the fiction resistance. Figure 11 shows the velocity distribution of the extrudate under the synthesized effects of eccentricity ratio (e=0.43), proper design of the second-step welding chamber, and uneven bearing length. By comparing Figs. 8c and 10, the velocity difference has been further decreased from 12.8 to 7.93 mm/s, and the SDV decreases from 2.63 to 2.18 mm/s. More importantly, the defects of twist and bending on extrudate have been almost eliminated, as shown in Fig. 11.

Based on the analysis about velocity distribution of the extrudate, the two-hole porthole die has been optimized accordingly. The route of finding the best location of the die orifice, appropriate shape of the second-step welding chamber, and utilization of uneven bearing length is effective for designing a high-performance multi-hole die, which can obtain a uniform velocity distribution and improve the product quality.

4.4 Material flow and temperature distribution

In this section, the material flow behavior and temperature distribution on the extrudate, which are also important aspects for extrusion process, were investigated in the optimal die. To have a better comprehension, the extrusion die with the eccentricity ratio of 0.62, without the second-step welding chamber and with identical bearing length, was considered to be the initial die design to make a comparison. Figure 12 presents the node particle tracking path in the regions of the welding chamber, bearing, and profile to reflect the material flow behavior in initial and optimal dies. One can see that in the optimal die, the streams become much more even without any bending when they flow out from the bearing and profile by comparing panels a and b of Fig. 12. Additionally, by comparing the enlarged area of Fig. 12, viz., parts a and b, it can be observed that in the optimized die, the distortion of streams has been relieved effectively. This is because the orientations of some streams were changed by the second-step welding chamber to flow into the area with lower velocity favorably. The mentioned evidence proves that a more rational behavior of material flow can be realized after some modifications on initial die.

The temperature distribution of the extrudate in the initial and optimal die is compared in Fig. 13. It can be seen that the temperature was overall and slightly enhanced for the optimal

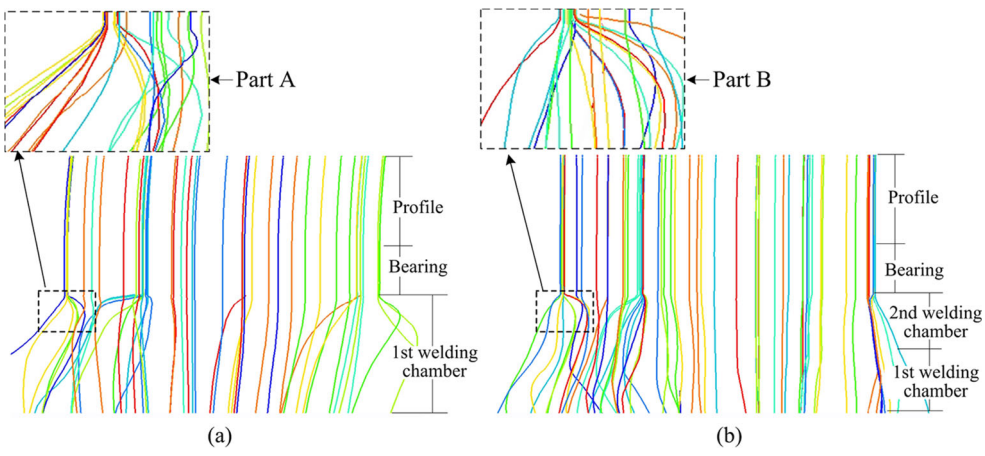

Fig. 12 The node particle tracking path in the welding chamber, bearing, and profile

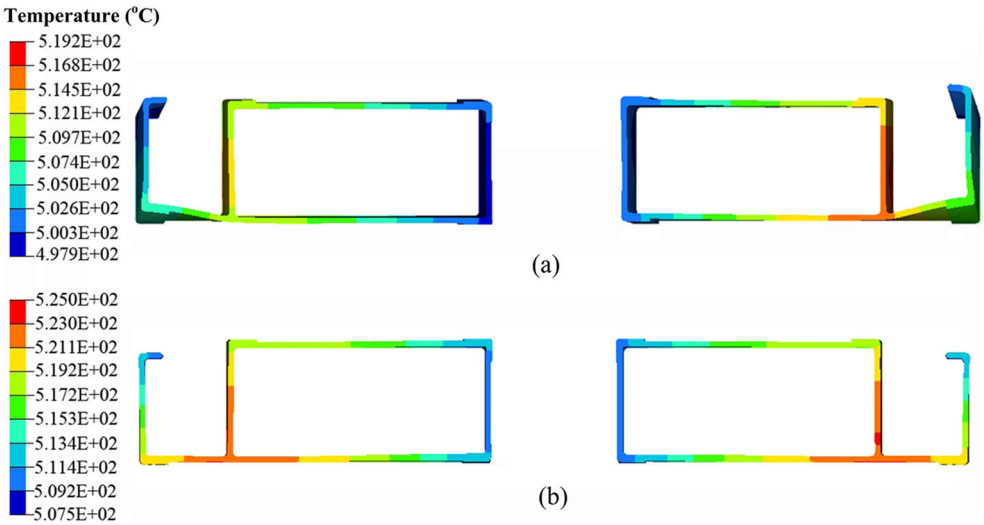

Fig. 13 Temperature distribution of the extrudate in the **a** initial die and **b** optimal die

die. The maximum temperature increases from 519.2 to 525.0 °C, and the minimum temperature increases from 497.9 to 507.5 °C. The reasons for this phenomenon are explained as follows. The utilization of the second-step welding chamber in the optimal die reduces the total space of the welding chamber. Therefore, the plastic deformation becomes severe in the regions of the welding chamber and leads to more heat generation. Moreover, the contact area between the material and colder die for heat dissipation is reduced. However, it should be pointed out that even the maximum temperature in the optimal die is still below the critical exit temperature of 540–590 °C for AA6063, and the overburning can be avoided. On the other hand, the temperature difference for the optimal die decreases from 21.3 to 17.5 °C, which is beneficial for reducing heat deformation of the extrudate. This decrease in temperature difference resulted from the more uniform material flow behavior controlled by the optimal die.

5 Conclusions

In the present study, the two-hole extrusion process for producing a hollow and thin-walled profile was modeled and simulated by means of the ALE method. The effects of eccentricity ratio, shape of the second-step welding chamber, and uneven bearing length on exit velocity distribution of extrudate were synthetically studied by analyzing and comparing the simulated results. Accordingly, a two-hole porthole die that can obtain a uniform velocity distribution and avoid the deflection of extrudate was designed. The important findings in this article are summarized as follows:

1. The location of die orifice was found to be an important aspect on affecting the velocity distribution of extrudate. The appropriate eccentricity ratio was determined to be 0.43 in this study, by which the fiction resistance on material flow resulting from vertical port bridge and porthole walls can be well balanced.
2. The well-designed second-step welding chamber of case 3 could effectively regulate the material flow more favorable to the regions with slow velocity. Furthermore, the uneven bearing length was utilized as the last step to balance the local material flow. With these modifications, the much more uniform material flow appeared with a SDV of 2.18 mm/s and the defects like twist or bending on extrudate were efficiently avoided.
3. The maximum temperature of 525.0 °C of the extrudate in the optimized die is lower than the critical exit temperature of AA6063, although the temperature was slightly increased because of the utilization of the second-step welding chamber. On the other hand, a better temperature distribution was obtained. Hence, the status of exit temperature of extrudate in the optimized die is acceptable.
4. A design route for multi-hole extrusion die of hollow and thin-walled profile was proposed to well control the flowing velocity at the bearing exit in this study. The main steps of the designed route consist of finding the best location of die orifice, appropriate shape design of the second-step welding chamber, and adjusting the bearing length. The present route should be quite helpful for die designers when facing this kind of problems in practical production.

Acknowledgments The authors would like to acknowledge the financial support from the National Natural Science Foundation of China (grant no. 51375270), the Fundamental Research Funds of Shandong University (grant no. 2014HW001), and the National Natural Science Foundation of China (grant no. 51105230).

Conflict of interest The authors declare that they have no conflict of interest.

References

1. Liu G, Zhou J, Duszczyk J (2008) FE analysis of metal flow and weld seam formation in a porthole die during the extrusion of a magnesium alloy into a square tube and the effect of ram speed on weld strength. J Mater Process Technol 200:185–198
2. Sinha MK, Deb S, Das R, Dixit US (2009) Theoretical and experimental investigations on multi-hole extrusion process. Mater Des 30: 2386–2392
3. Liu P, Xie S, Cheng L (2012) Die structure optimization for a large, multi-cavity aluminum profile using numerical simulation and experiments. Mater Des 36:152–160
4. Farjad Bastani A, Aukrust T, Brandal S (2011) Optimisation of flow balance and isothermal extrusion of aluminium using finite-element simulations. J Mater Process Technol 4:650–667
5. Duan X, Sheppard T (2003) Simulation and control of microstructure evolution during hot extrusion of hard aluminium alloys. Mater Sci Eng A 351:282–292
6. Wu X, Zhao G, Luan Y, Ma X (2006) Numerical simulation and die structure optimization of an aluminum rectangular hollow pipe extrusion process. Mater Sci Eng A 435:266–274
7. Wu CY, Hsu YC (2002) Optimal shape design of an extrusion die using polynomial networks and genetic algorithms. Int J Adv Manuf Technol 19:79–87
8. Zhou J, Li L, Duszczyk J (2004) Computer simulated and experimentally verified isothermal extrusion of 7075 aluminium through continuous ram speed variation. J Mater Process Technol 146:203–212
9. Duan X, Velay X, Sheppard T (2004) Application of finite element method in the hot extrusion of aluminium alloys. Mater Sci Eng A 369:66–75
10. Lof J, Blokhuis Y (2002) FEM simulations of the extrusions of complexed thin-walled aluminum sections. J Mater Process Technol 122:344–354
11. Jo HH, Lee SK, Jung CS, Kim BM (2006) A non-steady state FE analysis of Al tubes hot extrusion by a porthole die. J Mater Process Technol 173:223–231
12. Fang G, Zhou J, Duszczyk J (2009) Extrusion of 7075 aluminium alloy through double-pocket dies to manufacture a complex profile. J Mater Process Technol 209:3050–3059
13. Fang G, Zhou J, Duszczyk J (2008) Effect of pocket design on metal flow through single-bearing extrusion dies to produce a thin-walled aluminium profile. J Mater Process Technol 199:91–101
14. Kathirgamanathan P, Neitzert T (2009) Optimization of pocket design to produce a thin shape complex profile. Prod Eng Res Dev 3: 231–241
15. Chen H, Zhao G, Zhang C, Guan Y, Liu H, Kou F (2011) Numerical simulation of extrusion process and die structure optimization for a complex aluminum multicavity wallboard of high-speed train. Mater Manuf Process 26:1530–1538
16. Li F, Lin JF, Yuan J, Liu XJ (2009) Effect of inner cone punch on metal flow in extrusion process. Int J Adv Manuf Technol 42:489–496
17. Zhang CS, Zhao GQ, Chen H, Guan YJ, Kou FJ (2012) Numerical simulation and metal flow analysis of hot extrusion process for a complex hollow aluminum profile. Int J Adv Manuf Technol 60:101–110
18. Sun X, Zhao G, Zhang C, Guan Y, Gao A (2013) Optimal design of second-step welding chamber for a condenser tube extrusion die based on the response surface method and the genetic algorithm. Mater Manuf Process 28:823–834
19. Peng Z, Sheppard T (2004) Simulation of multi-hole die extrusion. Mater Sci Eng A 367:329–342
20. He YF, Xie SS, Cheng L, Huang GJ, Fu Y (2010) FEM simulation of aluminum extrusion process in porthole die with pockets. Trans Nonferrous Met Soc China 20:1067–1071
21. Ulysse P, Johnson RE (1998) A study of the effect of the process variables in unsymmetrical single-hole and multi-hole extrusion processes. J Mater Process Technol 73:213–225
22. Guan Y, Zhang C, Zhao G, Sun X, Li P (2012) Design of a multihole porthole die for aluminum tube extrusion. Mater Manuf Process 27: 147–153
23. Zhang C, Zhao G, Chen H, Guan Y, Cai H, Gao B (2012) Investigation on effects of die orifice lon three-hole porthole extrusion of Aluminum Alloy 6063 tubes. J Mater Eng Perform 22:1223–1232
24. Sinha MK, Deb S, Dixit US (2009) Design of a multi-hole extrusion process. Mater Des 30:330–334
25. Qamar SZ, Arif AFM, Sheikh AK (2004) A new definition of shape complexity for metal extrusion. J Mater Process Technol 155:1734–1739
26. Ganvir V, Lele A, Thaokar R, Gauthama BP (2009) Prediction of extrudate swell in polymer melt extrusion using an Arbitrary Lagrangian Eulerian (ALE) based finite element method. J Non-Newtonian Fluid Mech 156:21–28
27. Aymone JLF, Bittencourt E, Creus GJ (2001) Simulation of 3D metal-forming using an arbitrary Lagrangian-Eulerian finite element method. J Mater Process Technol 110:218–232
28. Zhang C, Zhao G, Chen H, Guan Y, Li H (2012) Optimization of an aluminum profile extrusion process based on Taguchi's method with S/N analysis. Int J Adv Manuf Technol 60:589–599
29. Ma X, de Rooij MB, Schipper DJ (2012) Friction conditions in the bearing area of an aluminium extrusion process. Wear 278:1–8